Published in final edited form as:
J Sep Sci. 2009 January ; 32(1): 44–56. doi:10.1002/jssc.200800474.

Extensive Fractionation and Identification of Proteins within Nasal Lavage Fluids from Allergic Rhinitis and Asthmatic Chronic Rhinosinusitis Patients

Linda M. Benson[1], **Christopher J. Mason**[1], **Oren Friedman**[2], **Hirohito Kita**[3], **H. Robert Bergen III**[1], and **Douglas A. Plager**[3]

[1]Mayo Proteomics Research Center, Research Laboratory, Mayo Clinic, Rochester, MN

[2]Department of Otorhinolaryngology, Research Laboratory, Mayo Clinic, Rochester, MN

[3]Allergic Diseases, Research Laboratory, Mayo Clinic, Rochester, MN

Abstract

Allergic rhinitis (AR), chronic rhinosinusitis (CRS), and asthma are prevalent airway diseases that can have a substantial impact on a patient's quality of life. Mass spectrometry analyses of biological fluids can effectively screen for proteins associated with disease processes, however, initial detection of diagnostic proteins is difficult due to protein complexity and dynamic range. To enhance the detection of lower abundance proteins, intact nasal lavage fluid (NLF) proteins from nonpolypoid AR and from asthmatic CRS patients were extensively fractionated prior to LC/MS/MS analysis. Pooled NLF samples were processed to remove low molecular weight molecules and high abundance plasma proteins. Anion exchange chromatography (AX) followed by RP-LC further separated the remaining intact NLF proteins. The resulting fractions were digested with trypsin and the peptides analyzed by LC/MS/MS. Spectra were searched with Mascot, Sequest, and X!Tandem to obtain peptide identifications and subsequently analyzed by Scaffold software to identify parent proteins with at least 99% confidence. The 197 identified proteins are compared to those previously cited in the literature and the workflow evaluated to determine the usefulness for detection of lower abundance proteins. This is the first extensive list of NLF proteins generated from CRS patients with coexisting asthma.

Keywords

Allergic rhinitis; Chronic rhinosinusitis; Nasal lavage; Protein fractionation; Proteomics

1 Introduction

Rhinitis and sinusitis comprise a large group of disorders that impact tens of millions of people in the U.S. and worldwide. Symptoms can range from mild rhinorrhea and sneezing in allergic rhinitis (AR) to debilitating mucus compaction and tissue remodeling in chronic rhinosinusitis (CRS). AR and CRS are separately associated with asthma, another prevalent and potentially debilitating airway disease [1]. Together, AR, CRS, and asthma, with their characteristic eosinophilic inflammation, account for tens of billions of annual costs [2,3]. Current therapeutic options can control mild AR and asthma, but more severe disease requires

Correspondance: Douglas A. Plager, PhD, Allergic Diseases Research Laboratory, Mayo Clinic, Guggenheim 4, 200 First Street SW, Rochester, MN 55905 USA, Plager.Douglas@mayo.edu, Tel: 507-284-9931, Fax: 507-284-5045.

continuous immunosuppressive therapy. For CRS, no standard FDA-approved therapy exists and endoscopic sinus surgery is a common last resort intervention.

Proteomic studies identify proteins using electrophoretic, chromatographic, and mass spectrometry techniques. Differential proteomics can be used to define biomarkers or molecular pathways associated with disease pathology. The serum proteome has been studied most frequently; however, other human proteomes, such as cerebrospinal fluid, saliva, urine, bronchoalveolar fluid, and nasal lavage fluid (NLF), are appearing in the literature [4,5]. There are four main components to a proteomic study: (1) sample collection and protein extraction, (2) protein or peptide fractionation, (3) detection of peptides or proteins, and (4) interpretation and protein identification. Experimental design and implementation are difficult as each of these components require optimization for individual proteomes; often times with limited sample numbers and protein quantities.

The complexity of biological fluids, dynamic range of the proteins, and the presence of high abundance proteins are problematic in proteomic studies but can be addressed by various fractionation techniques. Numerous gel-based and gel-free protein fractionation and multidimensional approaches exist; all have distinctive advantages and drawbacks. 2-DE gel fractionation has a limited dynamic range of proteins, thus decreasing detection of low abundance proteins, very small or large proteins, as well as basic and hydrophobic proteins. Gel-free approaches overcome the dynamic range problem and can be directly coupled to MS and automated for high throughput analysis. Commonly, two or more fractionation techniques are combined, either off-line or on-line with MS, to obtain adequate protein or peptide separation for detection of lower abundance proteins. Previous proteomic studies reveal the necessity for complementary multidimensional fractionation for more complete protein identification profiles.

Proteomic studies of NLF can provide essential information to understand the pathophysiologic pathways, determine diagnostic biomarkers, and design effective therapeutic treatments for rhinosinusitis conditions. Numerous techniques have been used to identify NLF proteins and determine differences associated with certain disease states or chemical exposures. Lindahl et al. identified several proteins in NLF using 2-DE in combination with western blotting or N-terminal sequencing [6-9] and more recently using 2-DE with MS to compare NLF proteins from healthy controls and epoxy workers exposed to dimethylbenzylamine [10,11], and from nonsmokers and smokers [12]. This group and that of Bryborn et al. [13] also used 2-DE with MS to compare NLF from healthy controls and AR patients [14]. Johannesson et al. used 2-DE and LC/MS/MS to identify NLF proteins that form adducts with hexahydrophthalic anhydride, a highly allergenic chemical [15], while Casado et al. used LC/MS/MS to compare protein profiles of sinusitis patients before and after antibiotic treatment [16]. In a follow-up study, protein profiles before and after nasal provocation identified several new proteins in NLF not previously observed by the 2-DE studies [17]. A recent review discusses the importance of separation techniques prior to MS analysis of NLF proteins [18], and Tewfik et al. used prefractionation and peptide labeling techniques to compare the nasal mucus proteins from CRS and control subjects [19]. Thus, these studies utilized a variety of proteomic techniques, and although the combined efforts identified numerous NLF proteins, no single workflow appeared to provide optimal protein identifications.

In this study, a combination of affinity, anion exchange (AX), and reverse phase separation techniques were used to extensively fractionate intact NLF proteins from AR or asthmatic CRS patients prior to digestion and LC/MS/MS analysis. Our main goal was to identify new, lower abundance proteins. Protein lists are presented along with discussion of the advantages and disadvantages of the experimental workflow.

2 Materials and Methods

2.1 Chemicals and reagents

Ammonium bicarbonate (NH_4HCO_3), DTT, trifluoroethanol (TFE), glacial acetic acid (HAc), formic acid, iodoacetamide (IA), and NaCl were purchased from Sigma-Alrich, (Milwaukee, WI), urea from Bio-Rad Laboratories (Hercules, CA), Zwittergent 316 (Z316) detergent from Calbiochem (San Diego, Ca), and sequencing grade modified trypsin from Promega Corporation (Madison, WI). Burdick and Jackson HPLC grade water and ACN were ordered from VWR International, Inc. (North Mankato, MN).

2.2 Sample collection

NLF samples were obtained from 9 and 6 patients diagnosed with nonpolypoid AR and CRS with coexisting asthma, respectively, after obtaining their informed consent and via an Institutional Review Board-approved protocol. Exclusion criteria included pregnancy or lactation or a history of smoking, immunodeficiency or cystic fibrosis, airway bacterial or viral infection, antibiotic therapy in the past week, systemic glucocorticoids in the past three months, or allergy immunotherapy in the past year. Intranasal medications, non-prescribed medications, or systemic medications to treat AR or CRS were stopped at least four days before and inhaled medications at least one day before NLF collection. Without breathing or swallowing by the subject and with their neck tilted 30 degrees back from the vertical, 5 mL of sterile isotonic saline was instilled into one nostril, a 10 second wait was observed, and the lavage solution was expelled into a collection beaker. The lavage solution was immediately transferred to a sterile conical tube and placed on ice. This was repeated for the other nostril. The ice-cold nasal lavage was gently rocked at room temperature for 15 minutes and then centrifuged at 800 x g for 10 min at 4° C. Nasal lavage supernatant, excluding pelleted cellular material and any buoyant mucus, was collected. Protein concentrations were determined on individual lavage supernatant samples by the Bradford assay (BSA reference standard; Bio-Rad Laboratories, Hercules, CA). Pooled samples for each group were prepared by combining 100 to 350 μg of protein from individual patients to provide a total protein content of 2 mg in 14.3 ml and 1.7 mg in 10.7 ml for AR and CRS NLF, respectively. Pooled samples were frozen at −80° C until fractionation.

2.3 Abundant plasma protein depletion

The pooled lavage samples were thawed, desalted, and concentrated using an iCON Concentrator (20 mL maximum volume and 9 kDa molecular weight cut-off (MWCO); Pierce, Rockford, IL) to ~200 μl. The retentate was diluted with Agilent Buffer A (Agilent Technologies; Wilmington, DE), filtered through an UltraFree-MC spin column (Millipore Corporation; Bedford, MA), and applied directly to a preconditioned Multiple Affinity Removal Column (MARS; 4.6×100 mm; HU6; Agilent Technologies) according to manufacture protocol. Samples were kept on ice or cooled in refrigerated centrifuges at all times. The collected flow-through depleted fraction was desalted, washed with 20 mM Tris, pH 8.2, concentrated to ~200 μl using an iCON Concentrator (7 mL; 9 kDa MWCO), and injected directly onto the AX column.

2.4 Anion exchange fractionation (AX)

AX was performed using a BioSuite Q-PEEK column (4.6 × 50 mm; 10μ; Waters Corporation; Milford, MA) on a 10AD*VP* HPLC system (Shimadzu Scientific Instruments; Columbia, MD). The entire desalted MARS depleted protein sample was loop injected directly onto the column. Mobile phase buffer composition was 20 mM Tris, pH 8.2 for buffer A and 20 mM Tris, pH 8.2 with 0.5 M NaCl for buffer B. Separation was achieved with a gradient of 0-50% B over 30 minutes; 50-100% B over 15 minutes; 100% B for 10 minutes; followed by 15 minutes of

re-equilibration at 0% B. The separation was monitored at 214 nm. One minute fractions were collected over 70 minutes (400 μl/min) and frozen at −80° C prior to reverse-phase separation.

2.5 Reverse-Phase fractionation (RP)

AX fractions were thawed and 190 μg of preweighed dry urea powder and 4 μl HAc added to each tube and incubated for 30 min at room temperature. RP separation was achieved on a Macroporous Reverse-Phase High Recovery Protein Column (mRP-C18; 2.1 × 75mm; 5μ; 80° C; Agilent Technologies; Foster City, CA) with mobile phases of 0.1% TFA in H_2O (pump A) and 0.08% TFA in ACN (pump B). The denatured AX fractions were loaded onto the column and washed for 6 minutes with mobile phase A prior to a separation gradient of 5-30% B over 17 minutes; 30-55% B over 20 minutes; 55-100% B over 10 minutes; 100% B over 10 minutes; followed by re-equilibration at 5% B for 13 minutes. Separation was achieved with a flow rate of 200 μl/min. One-minute fractions were collected and up to 5 fractions combined according to the 220 nm UV intensity (1357 AR fractions; 690 CRS fractions). All fractions were frozen, dried on a SpeedVac, and stored at −20° C.

2.6 Tryptic Digestion

RP fractions were reconstituted with 5 μl TFE and 25 μl 40 mM NH_4HCO_3. Proteins were reduced with 20 mM DTT and alkylated with 40 mM IA at room temperature for 1 hour. The fractions were diluted with NH_4HCO_3 buffer prior to addition of trypsin (0.5μg) and incubated overnight at 37° C. Digested fractions were dried and stored at −20° C until LC/MS/MS analysis.

2.7 LC/MS/MS analysis of peptides

Automated LC-MS/MS analyses were performed on a linear ion trap mass spectrometer (LTQ; ThermoFinnigan San Jose, CA) interfaced to a Paradigm MS4 autosampler and liquid chromatograph (Michrom BioResources Inc, Auburn,CA) using a 75μm × 10 cm ProteoPepII C_{18} PicoFrit nanoflow column (New Objective Inc, Woburn, MA). The 2047 digested fractions were reconstituted into 18 μl of sample buffer (98:2 H_2O:ACN; 0.1% formic acid; 0.0005% Z316) and 15 μl loaded onto a 250 nL OPTI-PAK trap (Optimize Technologies, Oregon City, OR) custom packed with Michrom Magic C_8 solid phase particles. (Michrom Bioresources, Auburn, CA). Mobile phase A consisted of water/formic acid (99.9/0.1 by volume) and mobile phase B of ACN/formic acid (99.9/0.1 by volume). The LC method employed a gradient of 5 to 60% B over 30 minutes, 60 to 80% B over 3 minutes, followed by re-eqilibrium at 5% B for 10 minutes, with a column flow of 0.300 ul/min. The ion trap experiment was set for data dependent triple play consisting of a full scan for ions in mass range of 400-1400 *m/z*, triggering to 10 amu profile mode zoom scan then MS/MS mode on the full scan ions with intensities exceeding a preset threshold of 2000 counts. The MS/MS spectra were aquired with a 2.5 mass unit isolation width, target ion population of 2×10^4 ions, two microscans, maximum ionization fill time of 200 ms, normalized collision energy of 35%, activation Q of 0.25, and activation time of 30 ms. Once ions were selected for MS/MS, they were subsequently excluded for 120 seconds allowing 2 repeats. The exclusion window was 1.5 mass units below and above the exclusion mass. The maximum scan time was ~0.9 seconds depending on the ion injection time automatically determined by the instrument. The MS/MS spectra obtained from the 1357 AR and 690 CRS fractions were combined into one AR and one CRS MS/MS data file and converted to DTA files using Bioworks software (version 3.2; ThermoFinnigan).

2.8 Data analysis and protein identification

The Ar and CRS DTA files were analyzed using Mascot (Matrix Science, London, UK; version 2.1.03), Sequest (ThermoFinnigan, San Jose, CA; version 27, rev. 12v) and X!Tandem (www.thegpm.org; version 2006.09.15.3). All three programs searched the

Sprot_20070320_human_r.fasta.hdr database; variable modifications included methionine oxidation and N-acetylation of terminus and cysteines. Tolerances of 2.0 Da (precursor) and 1.0 Da (fragment) were utilized while full tryptic cleavage was required and up to two missed cleavages allowed. Scaffold (version Scaffold-01_05_14, Proteome Software Inc., Portland, OR) was used to compile and assign probability scores. Peptide identifications were accepted if they could be established at greater than 95.0% probability as specified by the Peptide Prophet algorithm [20]. Protein identifications were accepted if they could be established at greater than 99.0% probability and contained at least 2 identified peptides. Protein probabilities were assigned by the Protein Prophet algorithm [21].

3 Results and discussion

The aim of this study was to obtain an extensive list of lower abundance proteins in NLF from nonpolypoid AR and from asthmatic CRS patients (Table 1). Identifying the proteins specific to NLF can be complicated by contaminating plasma proteins from lesions or capillary breakthrough into the nasal passages. The plasma proteins increase the complexity of NLF and make it difficult to detect lower abundance proteins. Our approach was to maximize the separation of intact NLF proteins prior to digestion to increase the number of peptides per protein detected and obtain more protein identifications. The individual techniques used in our protocol have been standardized by the manufacturers and other groups. To this end, we used a combination of affinity, AX, and RP chromatography prior to LC/MS/MS analysis of the digested peptides to identify proteins found in NLF from patients diagnosed with AR or CRS with coexisting asthma (Figure 1).

Because individual NLF samples had low protein concentrations compared to other biological fluids and variable protein concentrations and volumes (52 to 407 μg/mL and 2.5 to 8.0 mL among the 15 NLF samples), individual sample volumes providing 100 to 350 μg of protein were pooled to obtain a 2 mg (14.3 mL AR) or 1.7 mg (10.7 mL CRS) total protein preparation. Initial sample preparation included the use of iCON spin filters to reduce the volume and desalt the pooled NLF samples. The manufacturer claims >90% recovery of proteins using their suggested protocol. The iCON retentates were filtered through an Ultra-free spin column to clarify and remove particulates before injection onto the MARS column. The removal of the top six abundant plasma proteins (albumin, transferrin, IgG, IgA, anti-trypsin, haptoglobin; 85% total plasma protein; 99% efficiency) by the MARS column was important to offset the variability in the concentration of contaminating plasma proteins found in each individual NFL sample[22]. Figure 2A shows the elution profile of the AR NLF proteins off the MARS column. Peak 1 area shows that the majority of the proteins in the AR NFL sample were not retained on the column, whereas, Peak 2 area shows the contaminating plasma proteins that were retained and then eluted off the column. The volume from the depleted protein fraction (Peak 1; 2.5 mL) was reduced and desalted using a smaller volume iCON filter (7 mL). The initial large NLF volumes (14.3 and 10.7 ml) and the post MARS column volumes (2.5 ml) required spin filters with large surface areas, and even with extensive washes of the filters, protein losses were significant. Bradford analysis of the concentrated, desalted protein fractions prior to AX fractionation showed substantial reduction of protein with only 73% and 78% protein recovered for AR and CRS, respectively. Protease inhibitors were not used in order to minimize the complexity of the NLF, however, the formation of truncated and degradation products could have also contributed to a reduced recovery of intact proteins.

AX was chosen as the first chromatographic fractionation following MARS depletion due to its efficient protein separation and the minimal sample handling needed to prepare the fractions for the subsequent RP separation. The proteins were separated by charge using a salt gradient as described. Figure 2B shows the AX chromatogram obtained of the AR NLF proteins present in Peak 1 (Figure 2A) off the MARS column. Although some of the larger peaks eluted over

several minutes, 1 minute fractions were collected in order to maintain maximum separation of the low abundance proteins. The comparison of AX fractions AR20 and AR 31 fractions, highlighted in Figure 2B, was used as an example to demonstrate the overlap of proteins identified in distinct AX fractions.

The AX fractions were prepared for RP separation according to manufacturer protocol. Typically, recovery of proteins on RP columns is low due to the irreversible absorption onto the stationary phase (30-80% efficiency). The stationary phase of the mRP-C18 column was designed to minimize absorption resulting in better peak resolution and protein recovery (>98%) [23]. Figure 2C shows the differences in the UV absorbance profiles from the RP separations of the AX AR20 and AX AR31 fractions from Figure 2B. The UV intensities from each RP analysis determined whether adjacent fractions (up to five) were pooled together prior to trypsin digestion. This resulted in 1357 fractions for the AR sample and 690 fractions for the CRS sample. According to the UV absorbencies shown in Figure 2C, 10 and 17 RP fractions were collected from the example AX AR20 and AX AR31 fractions, respectively. Since a single protein may be found in adjacent RP fractions, the individual MS/MS spectra obtained from each RP fraction (n=10 and 17) were combined prior to protein identification to increase the number of peptide hits for each protein. The top 12 non-keratin identified proteins from these two AX fractions are listed in Table 2. Lactotransferrin and lipocalin were the most abundant proteins found in AX AR20 and AX AR31 fractions, respectively. The two AX fractions contained common proteins, (e.g. desmoplakin and zinc-α-2-glycoprotein), although the elution times differed by 11 minutes. The identified proteins also displayed a wide range of p*I*s not consistent with AX separation properties. These discrepancies may be explained by peak broadening effects from decreased resolution on the AX column or the presence of truncated or modified protein products which differ in size and p*I* from the native state protein. Covalent or noncovalent interactions between an AX bound protein and other proteins could also contribute to the unexpected range of p*I*s. Due to the overlap of proteins observed in both the AX and RP fractions, the MS/MS spectra obtained from the 1357 AR and 690 CRS fractions were combined into one AR and one CRS data file prior to protein identification.

The AX and RP fractionation methods were fast and provided extensive separation of the NLF proteins; however, the trypsin digestion of >2000 fractions was time consuming and proved to be the major drawback of the workflow. Two digestion issues were recognized. First, to maintain stability, the RP fractions were lyophilized and stored at −20° C, and while TFE was used to enhance solubility prior to digestion, protein recoveries may have varied, especially in tubes containing small amounts of protein. Second, the digestion protocol was manually prepared in batches (~200 fractions/day), and although the protocol was consistently applied, digestion efficiencies may have fluctuated.

LTQ-MS instrumentation was used for LC/MS/MS analysis because of its speed and sensitivity. In order to detect the maximum number of peptides, especially those found at low levels, a longer gradient was used. The automation of the instrument was advantageous in handling the large number of digest fractions (25 samples/day); however, the weeks needed to complete the analyses required the replacement of cartridges, columns, and silica tubing introducing more variables into the study.

As observed in Table 2, peptides from the same proteins were found in several RP fractions. As a result of protein overlap in both the AX and RP fractions, all of the individual MS/MS spectra were combined prior to peptide identification in order to enhance the number of peptide hits per protein and increase the confidence level of protein identifications. The implementation of the three search engines Mascot, Seaquest, and X!Tandem, provided a more comprehensive list; however, this required more time and computing power (~2.5 million MS/MS spectra). The initial protein lists generated by Scaffold included 202 and 163 protein hits for AR and

CRS NLF, respectively. Proteins identified by the reverse database were removed. Upon manual inspection of the remaining spectral data, it was noted that a number of the identified peptides with higher charge states (3+ or 4+) and molecular mass (>2500 Da) had poor quality or questionable MS/MS spectra and were also removed. The revised list included 156 and 129 proteins identified for AR and CRS NLF, respectively. Of the total proteins observed, 88 proteins were identified from both AR and CRS NLF. Figure 3 illustrates the number of unique peptides (two required per protein) and the number of total spectra used to identify the AR and CRS NLF proteins. The expectation from the extensive protein fractionation was an increase in the number of peptides detected for each protein; however, Figure 3A shows that over 50% of the AR and CRS proteins were identified from two to four unique peptides. The majority of proteins identified from 20 or more unique peptides were keratins or plasma proteins. Figure 3B shows the distribution of total spectra collected per identified protein. Each unique peptide could produce more than one spectrum due to peptide concentration and/or more than one peptide charge state. A majority of the proteins were identified using nine or fewer spectra; again, the keratins and plasma proteins constituted the higher numbers of total spectra.

Keratins are observed in proteomic studies, often as a result of sample preparation contamination, but can be present at high levels in NLF due to the airway mucosa environment. Table 3 lists the identified keratins. Of note is the large number of total spectra detected from the keratins which reduced the detection of lower level peptides. A similar problem was observed due to the presence of plasma proteins that were not depleted by the MARS column. Table 4 illustrates the higher level of these proteins in CRS NLF compared to AR NLF. This could be the result of a protocol problem, such as a poorly equilibrated MARS column, or more likely, denaturation or degradation of the plasma proteins in one or more of the individual CRS NLF samples. The increased levels of the MARS targeted proteins in the final depleted CRS NLF sample may have contributed to a decrease in the number of proteins identified compared to AR NLF.

Table 5 lists the remaining 138 AR and CRS NLF proteins identified in our study of which 41 have been identified in previous proteomic NLF studies. Of these 138 proteins, 52 were detected in both CRS and AR NLF, 25 in only CRS NLF, and 61 in only AR NLF. The number of unique peptides used for protein identification is also given in Table 5 for CRS and AR NLF, respectively. The extensive fractionation was expected to enhance the number of unique peptides detected per protein; however, 81 of the 138 proteins in CRS and/or AR NLF were identified with only 2 or 3 unique peptides. Although the effectiveness of our workflow can not be unequivocally determined, many of the peptides for these 81 proteins may have gone undetected without the fractionation prior to digestion.

While the validity of directly comparing the two protein lists obtained from AR and CRS NLF is suspect, there are some obvious differences. Five proteins, α-2-macroglobulin, actin, long palate, lung and nasal epithelium carcinoma-associated protein, myosin 1, and myosin 4, were identified from AR NLF with 16, 19, 13, 12, and 25 unique peptides, respectively, but were not observed in the asthmatic CRS NLF. Similarly, lipocalin and lactotransferrin were identified from AR NLF with 29 and 47 peptides, respectively, compared to the CRS NLF at 3 and 11 unique peptides, respectively. In contrast, semenogelin 1 and 2 were identified in asthmatic CRS NLF with 15 and 6 unique peptides, respectively, but were not observed in AR NLF. Future studies are needed to determine the significance of these differences and how these newly identified proteins may be associated with rhinosinusitis diseases.

4 Concluding Remarks

In this study, we contribute lists of 197 NLF proteins identified from patients with nonpolypoid AR or CRS with coexisting asthma. A portion of these proteins have been identified previously;

however, the newly identified proteins can be further studied to determine their association with rhinosinusitis disease and/or their potential as disease biomarkers. Although difficulties, mainly protein loss and manual digestion of numerous fractions, may limit the practicality of this exact work flow for future analyses of biological fluids, in general, extensive protein prefractionation appears to have increased our detection of lower abundance NFL proteins.

Acknowledgments

The authors wish to thank Melinda Miller for MARS depletion sample preparation; Kay Bachman, RN and Sharone Rustad, RN for assistance with patient recruitment and nasal lavage fluid collection; and Mrs. Diana Ayerhart for manuscript preparation. Funding provided by NIH R21 AI058208 and Mayo Foundation.

Abbreviations

AR	allergic rhinitis
CRS	chronic rhinosinusitis
NLF	nasal lavage fluid
AX	anion exchange
TFE	trifluoroethanol
HAc	glacial acetic acid
IA	iodoacetamide
MWCO	molecular weight cut off
MARS	multiple affinity removal column
mRP-C18	macroporous reverse-phase high recovery protein column
LTQ	linear ion trap

5 References

[1]. Smart BA. Clin. Rev. Allergy Immuno.l 2006;30:153–164.

[2]. Bukstein D, Kraft M, Liu AH, Peters SP. J. Allergy Clin. Immunol 2006;118:S1–15. [PubMed: 17027530]

[3]. Sasama J, Sherris DA, Shin SH, Kephart GM, Kern EB, Ponikau JU. Curr. Opin. Otolaryngol. Head Neck Surg 2005;13:2–8. [PubMed: 15654207]

[4]. Hu S, Loo JA, Wong DT. Proteomics 2006;6:6326–6353. [PubMed: 17083142]

[5]. Thongboonkerd, VE. Proteomics of Human Body Fluids Principals, Methods, and Applications. Springer; 2007.

[6]. Lindahl M, Stahlbom B, Tagesson C. Electrophoresis 1995;16:1199–1204. [PubMed: 7498167]

[7]. Lindahl M, Stahlbom B, Svartz J, Tagesson C. Electrophoresis 1998;19:3222–3229. [PubMed: 9932819]

[8]. Lindahl M, Stahlbom B, Tagesson C. Electrophoresis 1999;20:3670–3676. [PubMed: 10612294]

[9]. Lindahl M, Svartz J, Tagesson C. Electrophoresis 1999;20:881–890. [PubMed: 10344263]

[10]. Lindahl M, Stahlbom B, Tagesson C. Electrophoresis 2001;22:1795–1800. [PubMed: 11425234]

[11]. Lindahl M, Irander K, Tagesson C, Stahlbom B. Biomarkers 2004;9:56–70. [PubMed: 15204311]

[12]. Ghafouri B, Stahlbom B, Tagesson C, Lindahl M. Proteomics 2002;2:112–120. [PubMed: 11788998]

[13]. Bryborn M, Adner M, Cardell LO. Respir. Res 2005;6:118. [PubMed: 16236163]

[14]. Ghafouri B, Irander K, Lindbom J, Tagesson C, Lindahl M. J. Proteome Res 2006;5:330–338. [PubMed: 16457599]

[15]. Johannesson G, Lindh C, Nielsen J, Bjork B, Rosquist S, Jonsson B.Al. Toxicol. Appl. Pharmacol 2004;194:69–78. [PubMed: 14728981]

[16]. Casado B, Pannell LK, Viglio S, Iadarola P, Baraniuk JN. Electrophoresis 2004;25:1386–1393. [PubMed: 15174061]

[17]. Casado B, Pannell LK, Iadarola P, Baraniuk JN. Proteomics 2005;5:2949–2959. [PubMed: 15996010]

[18]. Casado B. Curr. Allergy Asthma Rep 2004;4:224–229. [PubMed: 15056405]

[19]. Tewfik MA, Latterich M, DiFalco MR, Samaha M. Am. J. Rhinol 2007;21:680–685. [PubMed: 18201447]

[20]. Keller A, Nesvizhskii AI, Kolker E, Aebersold R. Anal. Chem 2002;74:5383–5392. [PubMed: 12403597]

[21]. Nesvizhskii AI, Keller A, Kolker E, Aebersold R. Anal. Chem 2003;75:4646–4658. [PubMed: 14632076]

[22]. Mrozinski, P.; Haiying, C.; Zolotarjova, N.; Szafranski, C.; Barrett, W.; Bailey, J.; Boyes, B.; Agilent Technologies, Inc.. 2005. 5989-2881EN

[23]. Barrett, W.; Martosella, J.; Zolotarjova, N.; Yang, L.; Szafranski, C.; Nicol, G.; Agilent Technologies, Inc.. 2005.

[24]. Ghafouri B, Kihlstrom E, Stahlbom B, Tagesson C, Lindahl M. Biochem. Soc. Trans 2003;31:810–814. [PubMed: 12887311]

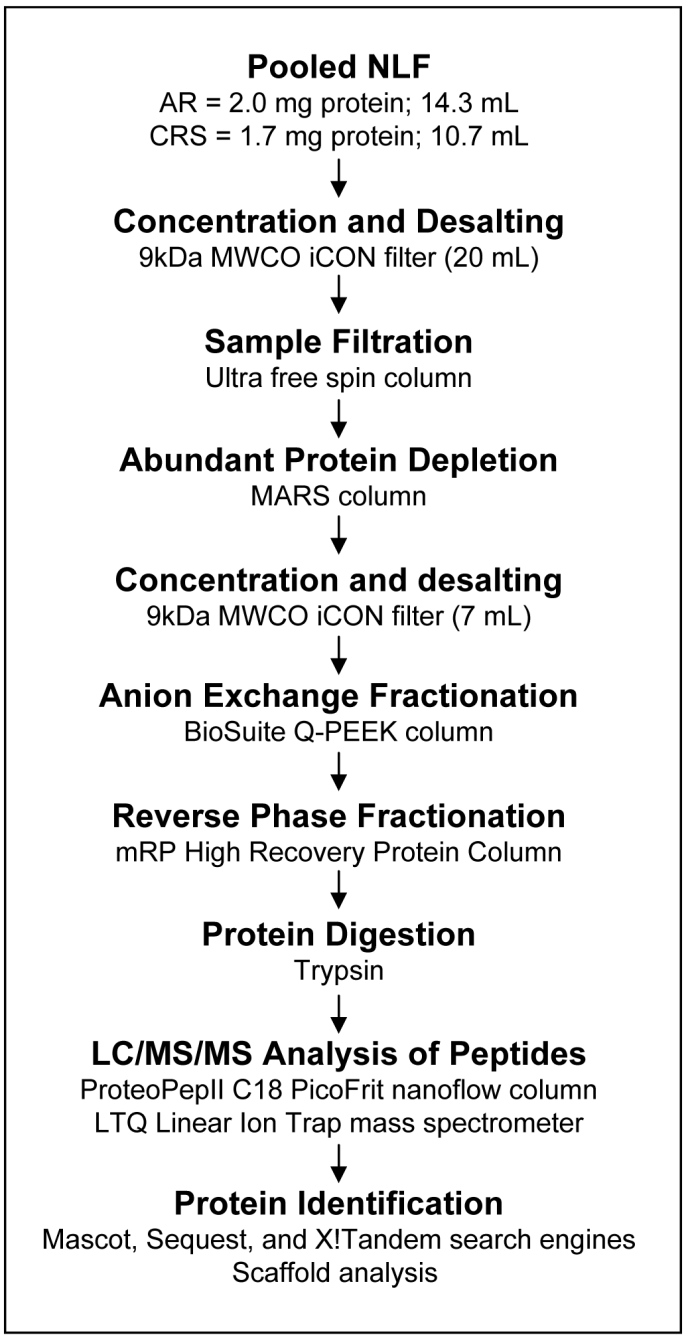

Figure 1. Workflow schematic

Pooled NLF sample proteins were concentrated, desalted, and extensively fractionated by affinity (MARS Column), anion exchange (BioSuite Q-PEEK Column), and RP (Macroporous RP High Recovery Protein Column) chromatography prior to LC/MS/MS analysis and protein identification from the tryptic peptides.

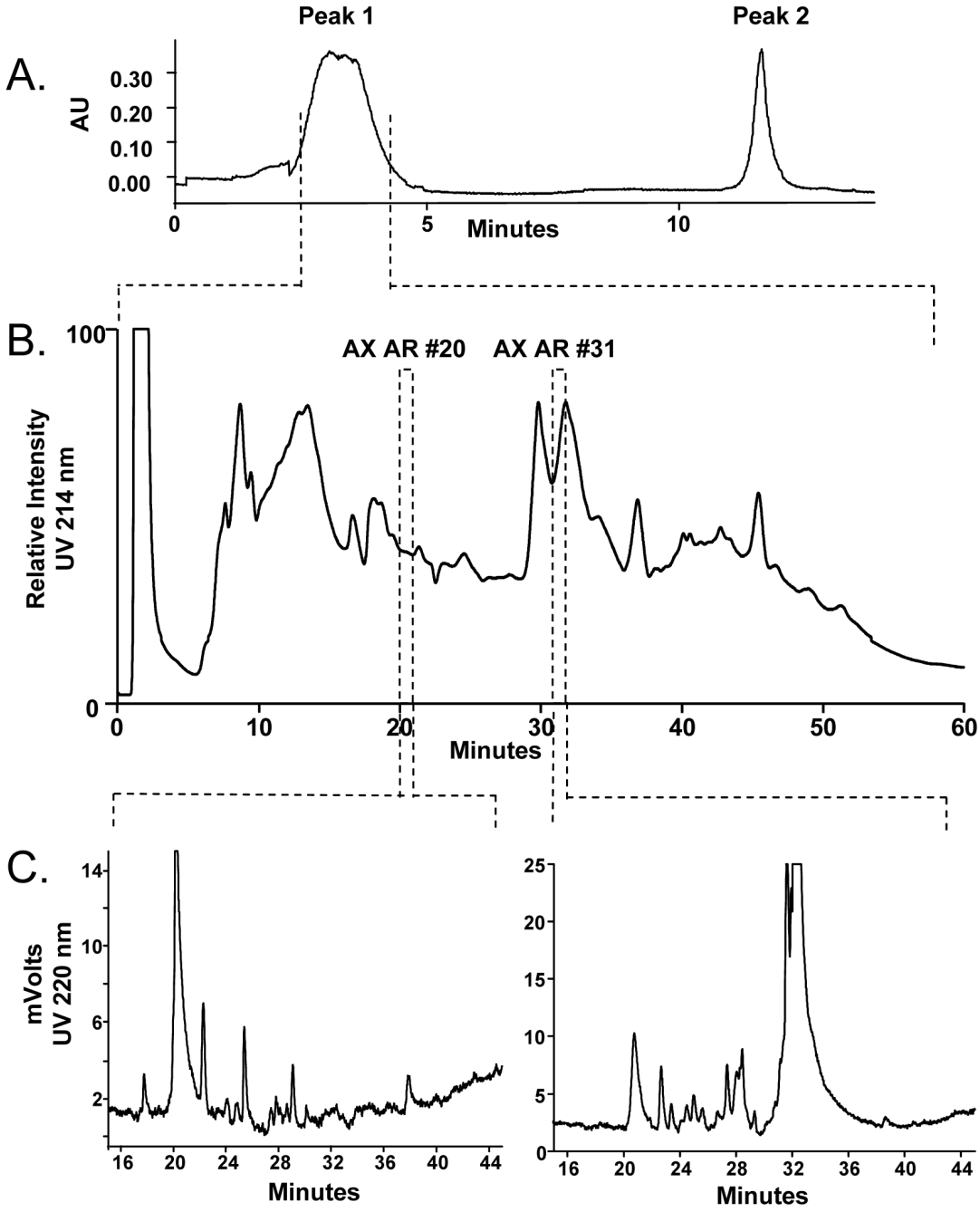

Figure 2. Chromatographic profiles of the pooled AR NLF sample

A.) Elution profile from the MARS column. Peak 1 is the fraction depleted of the six abundant plasma proteins. Peak 2 contains the bound plasma proteins. B.) The UV profile of separated Peak 1 proteins on the AX column using a salt gradient. One minute fractions were collected. C.) The UV profiles of AX fractions 20 and 31 on the mRP-C18 column. One to 5 minute fractions were collected for tryptic digestion.

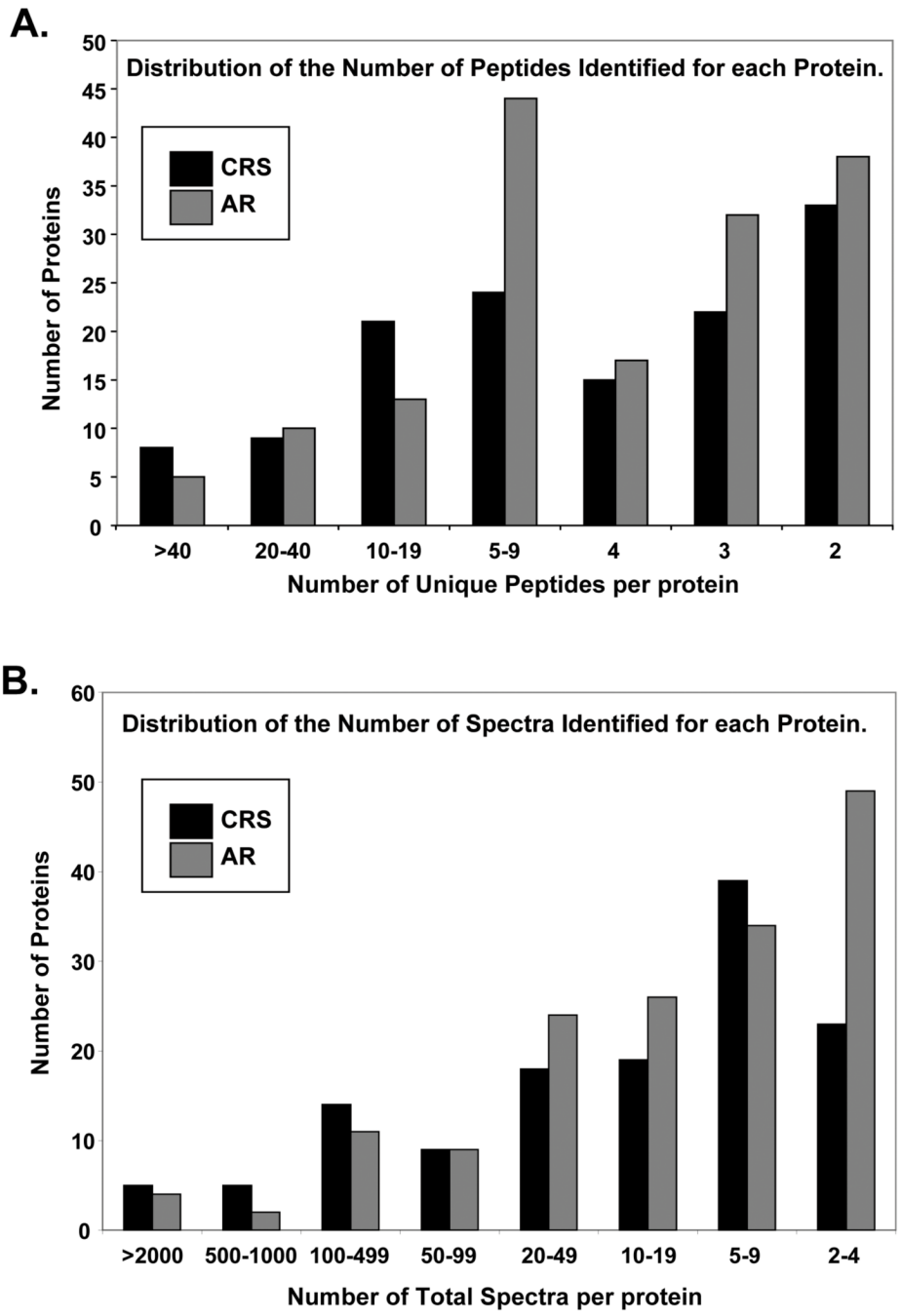

Figure 3. Distribution of the number of unique peptides and total spectra per protein for the CRS and AR proteins identified

A.) Over 50% of the proteins were identified from 2 to 4 unique peptides. Most proteins identified from 20 or more peptides were keratins or plasma proteins. B.) The distribution of total spectra ranged from 2 to >2000; the majority of proteins were identified from 9 or less spectra. Keratins and plasma proteins dominated the proteins with high spectral counts.

J Sep Sci. Author manuscript; available in PMC 2010 March 31.

Table 1

Demographics of Nasal Lavage Fluid Donors

NLF samples were obtained from 9 and 6 patients diagnosed with nonpolypoid AR and CRS with coexisting asthma, respectively. All subjects had limited confounding health issues and were off of AR- or CRS-related treatments before donating their NLF sample.

Sample ID	Age (yrs)	Sex	Race	Asthma dx*	Serum IgE**	Blood eosinophils (% / # x 10^9/L)	Aspirin sensitive	Nasal Polyps
AR								
1	37	F	unknown	No	+cat	1.41 / 0.12	No	No
2	24	F	Hispanic	No	++++HDM	1.68 / 0.10	No	No
3	25	F	unknown	No	+/−cat;+SRW;++Alt	2.16 / 0.11	No	No
4	22	F	White	No	+cat;++TG;++HDM	5.27 / 0.43	No	No
5	28	F	White	No	+HDM;++SRW	3.00 / 0.30	No	No
6	32	F	White	No	+SRW;++cat;++TG	3.27 / 0.28	No	No
7	38	F	White	No	− (patient reported oak)	5.46 / 0.46	unknown	No
8	34	F	White	No	+/−TG;+HDM;++SRW	unknown	No	No
9	20	M	White	No	+/−cat;+TG;++SRW;++HDM	2.90 / 0.19	No	No
CRS								
1	37	M	White	Yes	+cat;+SRW;+TG;+HDM;+++Alt	9.65 / 0.44	No	Yes
2	48	M	White	Yes	+/−TG;+Alt	1.66 / 0.12	No	Yes
3	33	M	White	Yes	−	6.66 / 0.50	No	No
4	45	F	White	Yes	− (patient reported horse hair)	4.89 / 0.40	No	Yes
5	33	M	White	Yes*	+/−cat;+SRW;+HDM	4.59 / 0.41	No	No
6	41	F	White	Yes	−	0.23 / 0.04	No	Yes

− = neg., <0.35; +/− = Equivocal, 0.35-0.70; + = 0.71-3.50, ++ = 3.51-17.5, +++ = 17.6-50, ++++ = 50.1-100 kU/L

* asthma diagnosis based primarily on a positive bronchial methacholine challenge test

** RAST tests for IgE specific for Cat Epithelium, Short Ragweed, Timothy Grass, House dust mite (DF), and Alternaria;

Table 2

Proteins identified from AR AX fractions 20 and 31

The top 12 non-keratin proteins from each fraction are ranked according to the number of unique peptides used for identification. Overlap of proteins and diversity in pIs may be due to protein degradation or noncovalent protein interactions.

	Protein accession number	SwissProt accession number	Protein name	Protein molecular weight (Da)	p*I*	Number of Unique Peptides
Allergic Rhinitus Anion Exchange Fraction #20						
1	TRFL_HUMAN	P02788	Lactotransferrin precursor	78164	8.47	22
2	SPB4_HUMAN	P48594	Serpin B4 (Squamous cell carcinoma antigen 2)	44837	5.86	9
3	DESP_HUMAN	P15924	Desmoplakin	331765	6.44	7
4	B2MG_HUMAN	P61769	Beta-2-microglobulin precursor	13696	6.07	5
5	S10A9_HUMAN	P06702	Protein S100-A9 (Calgranulin-B)	13224	5.71	5
6	ZA2G_HUMAN	P25311	Zinc-alpha-2-glycoprotein precursor	33854	5.58	5
7	SMR3A_HUMAN	Q99954	Submaxillary gland androgen-regulated protein	14100	10.35	4
8	SPR2B_HUMAN	P35325	Small proline-rich protein 2B	7956	8.81	4
9	SPB3_HUMAN	P29508	Serpin B3 (Squamous cell carcinoma antigen 1)	44547	6.35	4
10	ACTB_HUMAN	P60709	Actin, cytoplasmic 1	41719	5.29	4
11	S10A8_HUMAN	P05109	Protein S100-A8 (Calgranulin-A)	10816	6.51	4
12	TFF3_HUMAN	Q07654	Trefoil factor 3 precursor	8622	5.13	3
Allergic Rhinitus Anion Exchange Fraction #31						
1	LCN1_HUMAN	P31025	Lipocalin-1 precursor (Von Ebner gland protein)	19232	5.26	28
2	ZA2G_HUMAN	P25311	Zinc-alpha-2-glycoprotein precursor	33854	5.58	11
3	PROL4_HUMAN	Q16378	Proline-rich protein 4 precursor	15078	7.17	6
4	ACTC_HUMAN	P68032	Actin, alpha cardiac	42002	5.23	6
5	TFF3_HUMAN	Q07654	Trefoil factor 3 precursor	8622	5.13	5
6	TRFL_HUMAN	P02788	Lactotransferrin precursor	78164	8.47	5
7	LACRT_HUMAN	Q9GZZ8	Extracellular glycoprotein lacritin precursor	14228	5.17	3
8	WFDC2_HUMAN	Q14508	WAP four-disulfide core domain protein	12974	4.5	3
9	SMR3A_HUMAN	Q99954	Submaxillary gland androgen-regulated protein	14100	10.35	3

	Protein accession number	SwissProt accession number	Protein name	Protein molecular weight (Da)	p*I*	Number of Unique Peptides
10	TCO1_HUMAN	P20061	Transcobalamin-1 precursor	48177	4.85	3
11	DESP_HUMAN	P15924	Desmoplakin	331765	6.44	3
12	FABPE_HUMAN	Q01469	Fatty acid-binding protein, epidermal	15015	6.82	3

Table 3
Keratins identified from CRA and AR NLF

The number of unique peptides and total spectra used to identify keratins are noted for CRS and AR, respectively. The high numbers of total spectra from certain keratins interfere with the detection of lower abundance peptides.

	Protein accession number	Protein name	Number of unique peptides CRS, AR	Number of total spectra CRS, AR
1	K1C10_HUMAN	Keratin, type I cytoskeletal 10	50, 57	3195, 5280
2	K1C12_HUMAN	Keratin, type I cytoskeletal 12	0, 2	0, 2
3	K1C13_HUMAN	Keratin, type I cytoskeletal 13	12, 11	47, 20
4	K1C14_HUMAN	Keratin, type I cytoskeletal 14	23, 27	299, 330
5	K1C16_HUMAN	Keratin, type I cytoskeletal 16	30, 33	618, 427
6	K1C17_HUMAN	Keratin, type I cytoskeletal 17	18, 15	50, 64
7	K1C19_HUMAN	Keratin, type I cytoskeletal 19	0, 4	0, 5
8	K1C9_HUMAN	Keratin, type I cytoskeletal 9	59, 52	3130, 2271
9	K1H1_HUMAN	Keratin, type I cuticular Ha1	15, 16	142, 95
10	K1H2_HUMAN	Keratin, type I cuticular Ha2	4, 0	4, 0
11	K1H4_HUMAN	Keratin, type I cuticular Ha4	26, 19	148, 72
12	K1H5_HUMAN	Keratin, type I cuticular Ha5	11, 8	47, 22
13	K1H6_HUMAN	Keratin, type I cuticular Ha6	10, 5	39, 14
14	K1H7_HUMAN	Keratin, type I cuticular Ha7	3, 0	11, 0
15	K1H8_HUMAN	Keratin, type I cuticular Ha8	2, 4	2, 6
16	K1HB_HUMAN	Keratin, type I cuticular Ha3-II	0, 4	0, 16
17	K22E_HUMAN	Keratin, type II cytoskeletal 2 epi	70, 70	2566, 3057
18	K22O_HUMAN	Keratin, type II cytoskeletal 2 oral	3, 0	4, 0
19	K2C1_HUMAN	Keratin, type II cytoskeletal 1	77, 59	7115, 5954
20	K2C1B_HUMAN	Keratin, type II cytoskeletal 1b	2, 3	7, 10
21	K2C3_HUMAN	Keratin, type II cytoskeletal 3	7, 0	9, 0
22	K2C4_HUMAN	Keratin, type II cytoskeletal 4	6, 12	19, 19
23	K2C5_HUMAN	Keratin, type II cytoskeletal 5	33, 22	350, 230
24	K2C6A_HUMAN	Keratin, type II cytoskeletal 6A	44, 38	565, 504
25	K2C6B_HUMAN	Keratin, type II cytoskeletal 6B	9, 6	64, 26
26	K2C6D_HUMAN	Keratin, type II cytoskeletal 6D	2, 2	3, 4
27	K2C79_HUMAN	Keratin, type II cytoskeletal 79	0, 3	0, 4
28	KPRP_HUMAN	Keratinocyte proline-rich protein	15, 9	62, 21
29	KR101_HUMAN	Keratin-associated protein 10-1	0, 2	0, 3
30	KR103_HUMAN	Keratin-associated protein 10-3	2, 2	3, 4
31	KR132_HUMAN	Keratin-associated protein 13-2	3, 0	4, 0
32	KRA24_HUMAN	Keratin-associated protein 2-4	4, 3	30, 14
33	KRA43_HUMAN	Keratin-associated protein 4-3	0, 2	0, 2
34	KRA47_HUMAN	Keratin-associated protein 4-7	0, 2	0, 3
35	KRA49_HUMAN	Keratin-associated protein 4-9	2, 0	2, 0
36	KRA98_HUMAN	Keratin-associated protein 9-8	3, 0	4, 0

	Protein accession number	Protein name	Number of unique peptides CRS, AR	Number of total spectra CRS, AR
37	KRT33A_HUMAN	Keratin, Type I hair 3A	9, 8	26, 13
38	KRT33B_HUMAN	Keratin, Type I hair 3B	6, 0	19, 0
39	KRT81_HUMAN	Keratin type II cuticular Hb1	25, 24	154, 103
40	KRT82_HUMAN	Keratin type II cuticular Hb2	10, 4	57, 15
41	KRT83_HUMAN	Keratin type II cuticular Hb3	2, 4	9, 9
42	KRT84_HUMAN	Keratin type II cuticular Hb4	24, 7	69, 11
43	KRT85_HUMAN	Keratin type II cuticular Hb5	43, 25	229, 100
44	KRT86_HUMAN	Keratin type II cuticular Hb6	4, 3	13, 13

Table 4

Plasma proteins identified from CRS and AR NLF

The number of unique peptides and total spectra used to identify plasma proteins not retained on the MARS column are noted for CRS and AR, respectively. Denatured or modified proteins found in one or more individual NLF samples may have led to ineffective binding to the MARS column. The presence of plasma proteins is more evident in the CRS NLF compared to the AR NLF.

	Protein accession numbers	SwissProt accession number	Protein name	Number of unique peptides CRS,AR	Number of total spectr CRS,AR
1	A1AT_HUMAN	P01009	Alpha-1-antitrypsin precursor	22, 4	211, 6
2	ALBU_HUMAN	P02768	Serum albumin precursor	80, 34	3094, 118
3	HPT_HUMAN	P00738	Haptoglobin precursor	18, 0	188, 0
4	HPTR_HUMAN	P00739	Haptoglobin-related protein precursor	3, 0	12, 0
5	HV303_HUMAN	P01764	Ig heavy chain V-III region VH26 precursor	2, 0	4, 0
6	IGHA1_HUMAN	P01876	Ig alpha-1 chain C region	14, 6	334, 21
7	IGHA2_HUMAN	P01877	Ig alpha-2	3, 0	12, 0
8	IGHG1_HUMAN	P01857	Ig gamma-1 chain C region	14, 6	440, 17
9	IGHG2_HUMAN	P01859	Ig gamma-2 chain C region	4, 0	81, 0
10	IGHG3_HUMAN	P01860	Ig gamma-3 chain C region	2, 0	5, 0
11	IGHG4_HUMAN	P01861	Ig gamma-4 chain C region	2, 0	6, 0
12	IGJ_HUMAN	P01591	Immunoglobulin J chain	5, 0	23, 0
13	KAC_HUMAN	P01834	Ig kappa chain C region	7, 7	213, 13
14	LAC_HUMAN	P01842	Ig lambda chain C regions	4, 2	166, 4
15	TRFE_HUMAN	P02787	Serotransferrin precursor	58, 7	618, 10

Table 5

Protiens identified from CRS and AR NLF (minus the keratins and plasma proteins)

The number of unique peptides used for protein identification is given for CRS and AR NLF, respectively (>99% protein probability score with ≥2 peptides per protein). Of the 138 proteins listed, 81 were identified in CRS and/or AR NLF with only 2 or 3 unique peptides; 52 proteins were detected in both CRS and AR NLF, 25 in only CRS NLF, and 61 in only AR NLF. The proteins identified in previous studies are referenced.

	Protein Accession Number	SwissProt Accession Number	Protein Name	Molecular Weight	Number of Unique Peptides CRS,AR	Reference
1	1433B_HUMAN	P31946	14-3-3 protein beta/alpha	28065	0, 3	
2	1433S_HUMAN	P31947	14-3-3 protein sigma	27757	4, 4	
3	1433Z_HUMAN	P63104	14-3-3 protein zeta/delta	27728	3, 0	
4	A1AG1_HUMAN	P02763	Alpha-1-acid glycoprotein 1 precursor	23494	2, 0	[6,7,10,19]
5	A2MG_HUMAN	P01023	Alpha-2-macroglobulin precursor	163258	0, 16	[7,10,11,17]
6	AACT_HUMAN	P01011	Alpha-1-antichymotrypsin precursor	47635	5, 0	[6,16]
7	ACTA_HUMAN	P62736	Actin, aortic smooth muscle	41992	0, 19	[17]
8	ACTB_HUMAN	P60709	Actin, cytoplasmic 1	41720	7, 8	[13,16,17]
9	ACTN3_HUMAN	Q08043	Alpha-actinin-3	103279	0, 3	
10	ACTS_HUMAN	P68133	Actin, alpha skeletal muscle	42034	0, 2	
11	AL3A1_HUMAN	P30838	Aldehyde dehydrogenase, dimeric NADP-preferring	50361	0, 2	[17]
12	ALDOA_HUMAN	P04075	Fructose-bisphosphate aldolase A	39403	2, 6	
13	AMYC_HUMAN	P19961	Alpha-amylase 2B precursor	57692	2, 0	[19]
14	AMYS_HUMAN	P04745	Salivary alpha-amylase precursor	57750	0, 3	
15	ANXA1_HUMAN	P04083	Annexin A1	38697	4, 5	[7,9,10,12,16]
16	ANXA2_HUMAN	P07355	Annexin A2	38588	9, 7	[17]
17	APOA1_HUMAN	P02647	Apolipoprotein A-I precursor	30760	0, 4	[7,10,12-14,16,17,24]
18	APRV1_HUMAN	Q53RT3	Retroviral-like aspartic protease 1 precursor	36973	3, 0	
19	ARGI1_HUMAN	P05089	Arginase-1	34718	0, 3	
20	AT2A1_HUMAN	O14983	Sarcoplasmic/endoplasmic	110236	0, 4	

	Protein Accession Number	SwissProt Accession Number	Protein Name	Molecular Weight	Number of Unique Peptides CRS,AR	Reference
			reticulum calcium ATPase 1			
21	ATPA_HUMAN	P25705	ATP synthase subunit alpha, mitochondrial pre	59734	0, 5	
22	ATPB_HUMAN	P06576	ATP synthase subunit beta, mitochondrial precursor	56542	0, 7	
23	B2MG_HUMAN	P61769	Beta-2-microglobulin precursor	13697	2, 5	[12,14,17]
24	BLMH_HUMAN	Q13867	Bleomycin hydrolase	52544	0, 2	
25	CALL5_HUMAN	Q9NZT1	Calmodulin-like protein 5	15903	10, 8	
26	CALM_HUMAN	P62158	Calmodulin (CaM)	16820	2, 0	
27	CASPE_HUMAN	P31944	Caspase-14 precursor	27662	3, 3	
28	CF058_HUMAN	Q6P5S2	Uncharacterized protein C6orf58 precursor	37909	0, 2	
29	CO1A1_HUMAN	P02452	Collagen alpha-1(I) chain precursor	138893	7, 3	
30	CO1A2_HUMAN	P08123	Collagen alpha-2(I) chain precursor	129271	5, 0	
31	CO3_HUMAN	P01024	Complement C3 precursor	187131	0, 7	[7,10,16,17]
32	COF1_HUMAN	P23528	Cofilin-1	18485	0, 4	
33	CP343_HUMAN	Q9HB55	Cytochrome P450 3A43	57655	2, 0	
34	CYC_HUMAN	P99999	Cytochrome c	11731	0, 2	
35	CYTA_HUMAN	P01040	Cystatin-A	10989	4, 6	
36	CYTB_HUMAN	P04080	Cystatin-B	11121	2, 0	
37	CYTM_HUMAN	Q15828	Cystatin-M precursor	16493	0, 2	
38	CYTN_HUMAN	P01037	Cystatin-SN precursor	16343	0, 2	[10,12,13]
39	CYTS_HUMAN	P01036	Cystatin-S precursor	16197	4, 0	[8,10,12-14,19,24]
40	DCD_HUMAN	P81605	Dermcidin precursor	11266	5, 5	
41	DEF1_HUMAN	P59665	Neutrophil defensin 1 precursor	10183	3, 3	
42	DESP_HUMAN	P15924	Desmoplakin	331763	26, 26	
43	DMBT1_HUMAN	Q9UGM3	Deleted in malignant brain tumors 1 protein precursor	260707	0, 5	[17]

	Protein Accession Number	SwissProt Accession Number	Protein Name	Molecular Weight	Number of Unique Peptides CRS,AR	Reference
44	DSC1_HUMAN	Q08554	Desmocollin-1 precursor	100028	0, 2	
45	DSG1_HUMAN	Q02413	Desmoglein-1 precursor	113699	8, 12	
46	EF1A1_HUMAN	P68104	Elongation factor 1-alpha 1	50123	5, 4	
47	EF2_HUMAN	P13639	Elongation factor 2	95322	0, 2	
48	ENOA_HUMAN	P06733	Alpha-enolase	47152	6, 6	[13]
49	EPIPL_HUMAN	P58107	Epiplakin	553070	0, 3	
50	FABPE_HUMAN	Q01469	Fatty acid-binding protein, epidermal	15146	9, 5	
51	FETUA_HUMAN	P02765	Alpha-2-HS-glycoprotein precursor	39305	3, 0	[6,7,10]
52	FILA_HUMAN	P20930	Filaggrin	435127	18, 6	
53	G3P_HUMAN	P04406	Glyceraldehyde-3-phosphate dehydrogenase	36035	10, 5	
54	G3PT_HUMAN	O14556	Glyceraldehyde-3-phosphate dehydrogenase	44482	0, 3	
55	GRP78_HUMAN	P11021	78 kDa glucose-regulated protein precursor	72316	0, 2	
56	GSTP1_HUMAN	P09211	Glutathione S-transferase P	23339	3, 2	
57	H2A2A_HUMAN	Q6FI13	Histone H2A type 2-A	14078	0, 2	[16]
58	H4_HUMAN	P62805	Histone H4	11349	3, 5	[16,17]
59	HBA_HUMAN	P69905	Hemoglobin subunit alpha	15240	8, 0	[17,19]
60	HBB_HUMAN	P68871	Hemoglobin subunit beta	15980	6, 3	[13,17,19]
61	HEMO_HUMAN	P02790	Hemopexin precursor	51658	0, 6	[6,7,10,13]
62	HORN_HUMAN	Q86YZ3	Hornerin	282354	24, 8	
63	HPTR_HUMAN	P00739	Haptoglobin-related protein precursor	38990	3, 0	
64	HS90A_HUMAN	P07900	Heat shock protein HSP 90-alpha	84645	0, 2	
65	HSPB1_HUMAN	P04792	Heat-shock protein beta-1	22765	4, 5	
66	INVO_HUMAN	P07476	Involucrin	68447	2, 0	
67	KAD2_HUMAN	P54819	Adenylate kinase isoenzyme 2, mitochondrial	26461	0, 2	
68	KCRM_HUMAN	P06732	Creatine kinase M-type	43083	0, 3	

	Protein Accession Number	SwissProt Accession Number	Protein Name	Molecular Weight	Number of Unique Peptides CRS,AR	Reference
69	KPYM_HUMAN	P14618	Pyruvate kinase isozymes	57920	4, 3	
70	LACRT_HUMAN	Q9GZZ8	Extracellular glycoprotein lacritin precursor	14228	2, 5	[16]
71	LCN1_HUMAN	P31025	Lipocalin-1 precursor	19232	3, 29	[8,10,12-17,19,24]
72	LDHA_HUMAN	P00338	L-lactate dehydrogenase A chain	36671	3, 0	
73	LEG7_HUMAN	P47929	Galectin-7	15057	6, 10	
74	LMNA_HUMAN	P02545	Lamin-A/C	74123	2, 2	
75	LPLC1_HUMAN	Q8TDL5	Long palate, lung and nasal epithelium carcinoma-associated protein 1 pre	52442	0, 13	[17]
76	LYSC_HUMAN	P61626	Lysozyme C precursor	16518	4, 7	[7,10,12,14,17,19]
77	MDHM_HUMAN	P40926	Malate dehydrogenase, mitochondrial precursor	35513	0, 3	
78	MUC_HUMAN	P01871	Ig mu chain C region	49538	2, 0	
79	MUC5B_HUMAN	Q9HC84	Mucin-5B precursor	590465	0, 5	[17,19]
80	MYG_HUMAN	P02144	Myoglobin	17166	2, 3	
81	MYH1_HUMAN	P12882	Myosin-1	223103	0, 12	
82	MYH13_HUMAN	Q9UKX3	Myosin-13	223667	2, 0	
83	MYH2_HUMAN	Q9UKX2	Myosin-2	223032	0, 4	
84	MYH4_HUMAN	Q9Y623	Myosin-4	223000	0, 25	
85	MYH6_HUMAN	P13533	Myosin-6	223677	0, 2	
86	MYH9_HUMAN	P35579	Myosin-9	226520	2, 3	
87	NGAL_HUMAN	P80188	Neutrophil gelatinase-associated lipocalin pre	22570	0, 2	[17]
88	PDLI5_HUMAN	Q96HC4	PDZ and LIM domain protein 5	63953	0, 3	
89	PGAM1_HUMAN	P18669	Phosphoglycerate mutase 1	28786	0, 2	
90	PGK1_HUMAN	P00558	Phosphoglycerate kinase 1	44597	0, 3	
91	PIGR_HUMAN	P01833	Polymeric-immunoglobulin receptor precursor	83295	19, 9	[16,17,19]

	Protein Accession Number	SwissProt Accession Number	Protein Name	Molecular Weight	Number of Unique Peptides CRS,AR	Reference
92	PIP_HUMAN	P12273	Prolactin-inducible protein precursor	16555	10, 4	[10,12-15,17,24]
93	PKP1_HUMAN	Q13835	Plakophilin-1	82845	3, 3	
94	PLAK_HUMAN	P14923	Junction plakoglobin	81613	16, 13	
95	PLUNC_HUMAN	Q9NP55	Protein Plunc precursor	26696	2, 7	[10,12,14,17, 24]
96	PRB2_HUMAN	P02812	Basic salivary proline-rich protein 2	37259	3, 3	
97	PRB3_HUMAN	Q04118	Basic salivary proline-rich protein 3 precursor	30917	3, 6	
98	PRB4S_HUMAN	P10163	Basic salivary proline-rich protein 4 allele S precursor	25089	0, 2	
99	PRDX1_HUMAN	Q06830	Peroxiredoxin-1	22092	0, 2	
100	PRDX2_HUMAN	P32119	Peroxiredoxin-2	21874	2, 0	
101	PROL4_HUMAN	Q16378	Proline-rich protein 4 precursor	15106	0, 6	[16,17]
102	PRPC_HUMAN	P02810	Salivary acidic proline-rich phosphoprotein 1/2 pre	16998	2, 3	
103	S10A6_HUMAN	P06703	Protein S100-A6	10162	0, 2	
104	S10A7_HUMAN	P31151	Protein S100-A7	11440	10, 7	[13]
105	S10A8_HUMAN	P05109	Protein S100-A8	10817	6, 3	[14,19]
106	S10A9_HUMAN	P06702	Protein S100-A9	13224	7, 4	[10-14, 16,19,24]
107	S10AB_HUMAN	P31949	Protein S100-A11	11723	2, 0	
108	SEMG1_HUMAN	P04279	Semenogelin-1 precursor	52112	15, 0	
109	SEMG2_HUMAN	Q02383	Semenogelin-2 precursor	65425	6, 0	
110	SH3L3_HUMAN	Q9H299	SH3 domain-binding glutamic acid-rich-like pro	10419	0, 2	
111	SMR3A_HUMAN	Q99954	Submaxillary gland androgen-regulated protein 3 homolog A precursor	14100	0, 4	
112	SPB12_HUMAN	Q96P63	Serpin B12	46260	2, 0	
113	SPB3_HUMAN	P29508	Serpin B3	44548	15, 9	[17]
114	SPB4_HUMAN	P48594	Serpin B4	44837	7, 5	

	Protein Accession Number	SwissProt Accession Number	Protein Name	Molecular Weight	Number of Unique Peptides CRS,AR	Reference
115	SPR1A_HUMAN	P35321	Cornifin-A	9864	3, 2	
116	SPR1B_HUMAN	P22528	Cornifin-B	9869	2, 0	
117	SPR2B_HUMAN	P35325	Small proline-rich protein 2B	7957	4, 2	
118	SPR2G_HUMAN	Q9BYE4	Small proline-rich protein 2G	8139	0, 3	
119	STAT_HUMAN	P02808	Statherin precursor	7286	0, 2	[10,11,14,24]
120	TBA1_HUMAN	P68366	Tubulin alpha-1 chain	49906	0, 4	
121	TBA3_HUMAN	Q71U36	Tubulin alpha-3 chain	49877	3, 0	
122	TBB2A_HUMAN	Q13885	Tubulin beta-2A chain	49889	0, 4	
123	TCO1_HUMAN	P20061	Transcobalamin-1 precursor	48177	0, 3	[17,19]
124	TFF3_HUMAN	Q07654	Trefoil factor 3 precursor	8622	0, 7	
125	TGM3_HUMAN	Q08188	Protein-glutamine gamma-glutamyltransferase E pre	76615	3, 2	
126	THIO_HUMAN	P10599	Thioredoxin	11719	0, 2	
127	TNNT3_HUMAN	P45378	Troponin T, fast skeletal muscle	31807	0, 2	
128	TPIS_HUMAN	P60174	Triosephosphate isomerase	26651	4, 3	
129	TPM1_HUMAN	P09493	Tropomyosin-1 alpha chain	32692	0, 7	
130	TRFL_HUMAN	P02788	Lactotransferrin precursor	78164	11, 47	[7,10,12,14-17,19]
131	TYB4_HUMAN	P62328	Thymosin beta-4	5034	0, 3	
132	TYPH_HUMAN	P19971	Thymidine phosphorylase precursor	49937	0, 3	
133	U773_HUMAN	Q96DA0	Protein UNQ773/PRO1567 precursor	19582	0, 6	
134	UBIQ_HUMAN	P62988	Ubiquitin	8547	4, 2	
135	UTER_HUMAN	P11684	Uteroglobin precursor	9976	0, 3	[7,9,10,11,19,24]
136	VIME_HUMAN	P08670	Vimentin	53635	2, 0	
137	WFDC2_HUMAN	Q14508	WAP four-disulfide core domain protein 2 precursor	12974	0, 6	[15]
138	ZA2G_HUMAN	P25311	Zinc-alpha-2-glycoprotein precursor	33854	10, 13	[10,12,13,16,17,19]

J Sep Sci. Author manuscript; available in PMC 2010 March 31.